Experimentally Calibrated Thermal Stator Modelling of AC Machines for Short-Duty Transient Operation

Jonathan Godbehere
Student Member, IEEE
University of Bristol
Queen's Building,
University Walk,
Bristol, BS8 1TR, U.K
jg7560@bristol.ac.uk

Rafal Wrobel
Senior Member, IEEE
University of Bristol
Queen's Building,
University Walk,
Bristol, BS8 1TR, U.K
R.Wrobel@bristol.ac.uk

David Drury
University of Bristol,
Queen's Building,
University Walk,
Bristol, BS8 1TR, U.K
D.Drury@bristol.ac.uk

Phil H. Mellor
Member, IEEE
University of Bristol,
Queen's Building,
University Walk,
Bristol, BS8 1TR, U.K
P.H.Mellor@bristol.ac.uk

***Abstract* -- This paper presents an approach to the thermal design of an AC machine where the application requires low-duty transient operation. To provide accurate temperature predictions the design process has been informed with experimental data from tests on a stator-winding sector (motorette). These have been shown to be a time and cost-effective means of calibrating the thermal model of a full machine assembly, prior to manufacture of the final design. Such an approach is usually adopted in design analysis of machines with a concentrated winding topology. Here, the motorette testing has been extended to a machine with a distributed winding.**

Several alternate slot liner and impregnating materials have been evaluated to maximise the heat transfer from the winding body into the machine periphery, a total of nine stator section samples have been manufactured and tested. The performance trade-offs between the various combinations are discussed in detail, alongside their ability to satisfy the design requirements. Based upon these experimental results, the most promising designs have been selected for transient duty analysis against the design specification. A lumped parameter thermal model has been used for this purpose, calibrated using the data from the sub-assembly testing. Experimental results on the full machine assembly are presented, showing good correlation with the motorette calibrated thermal model.

***Index Terms*--AC machines, motorette assembly, lumped parameter thermal model, permanent magnet machines, short-duty transient operation, thermal design.**

I. INTRODUCTION

With the drive to produce more power dense and efficient electrical machines, accurate thermal modelling is becoming an increasingly important aspect of the design process. The ability to predict thermal behaviour in simulation is highly desirable; in order to reduce the overall design cycle by producing an optimised machine with the first prototype iteration.

Lumped parameter thermal models are a commonly used approach to analyse and predict electrical machine thermal behaviour [1–8], particularly when considering a transient duty [9], [10]. This is predominantly because of the fast computation time of lumped parameter circuits, which is necessary when evaluating performance over extended duty cycles. However critical parameters of these thermal models are difficult to predict without experimental calibration, for example the stator to slot liner interface, stator to housing interface, convection coefficient of the housing, and impregnation 'goodness' inside the slot [11–15]. This data can be sourced from experience with similar machines or previous iterations of the design. This approach is not applicable to the design of a new or unfamiliar machine topology where there is an absence of prior thermal data. However the manufacture of a prototype full stator assembly, for the purpose of calibrating the thermal analysis, can be costly and time consuming.

The approach adopted here is to obtain the required thermal calibration from tests on stator sub-assemblies, referred to as 'motorettes' [16–21]. A motorette is a representative sub-assembly of the stator and winding, manufactured using materials and processes commonly used in construction of the final electrical machine prototype. The thermal behaviour of the complete winding and stator periphery can be extrapolated from the motorette sample measurements. The motorette sub-assemblies are less costly and easier to prototype, allowing multiple batches to be produced and compared. This provides the opportunity to trial combinations of alternative materials to be used in the construction and assembly of the winding. As has been reported in the literature, the influence of the impregnation compound [22] and slot liner [23] have a significant impact on the thermal behaviour of a machine.

In this paper the approach is demonstrated in the design of an electrical machine for an electro-mechanical actuation application. The specification requires a low speed, high torque and low-duty transient operation. The two most important design objectives are torque density and compatibility with a zero-speed injection based sensorless position control. The sensorless position control criteria dictates a distributed winding, whereas the high torque density requires a high electrical loading and a large aspect ratio (stator outer diameter to machine active length), resulting in a proportionally large end winding region compared to the active length. The nature of the low speed, high torque application means that the losses in the machine are dominated by those from the winding. Further the total enclosed nature of the design results in the winding being cooled via the slot and this thermal interface is a critical factor. The optimisation

methodology used to generate the machine design is published in [24], [25], and initial motorette investigation in [26].

Motorette sub-assembly testing suits a single layer concentrated windings, since a coil wound around a single tooth is a direct replication of the winding. A full replication of a distributed winding as a stator segment is more challenging. Careful consideration must be given as to how to construct the motorette so that it represents the volume and lay of winding conductors found in the complete machine as close as possible. As part of the design study presented in this paper a thermal investigation into alternative slot insulation systems has been undertaken. A total of nine motorettes have been produced to the same geometry. Three different impregnation materials have been compared, including a solvent based varnish, a non-solvent based varnish, and an epoxy resin potting compound. Also compared are three different types of slot liner, producing nine different combinations of impregnation material and slot liner type. The different viscosities of varnishes and potting compounds effect the degree of penetration of the impregnation material within the slot liner [23], and is difficult to predict the resultant thermal properties without experimental data. The insight gained from this study has been used to downselect the insulation system for the final machine prototype. The measured data from tests on the complete machine prototype show good correlation with the prediction.

The paper has been organised in the following manner. Details of the machine specification and selected machine topology are presented in II. The motorette design and manufacture is presented in III. The motorette experimental setup is discussed in IV, with results shown in V. Section VI details the thermal model calibration process and thermal predictions for the complete machine assembly. Section VII introduces the manufactured prototype and experimental results on it. And finally, conclusions are presented in part VIII.

II. Machine Topology and Specification

The design considered in this paper is based on a high pole number 'V-shape' interior permanent magnet (V-IPM) topology. The winding is distributed across multiple parallel sided slots and cooled externally by natural convection. The requirements for the operating envelope are shown in Table I.

TABLE I
MACHINE OPERATING ENVELOPE SPECIFICATIONS

Peak Power (kW)	Peak Torque (Nm)	Maximum Speed (RPM)	Rated Current (A_{rms})	Peak Current (A_{rms})
1.5	47	420	15	65

The principal parameters describing the machine topology and geometry of the design are given in Table II. Active materials include round aluminium conductors, 42 MGOe NdFeB permanent magnets and 0.2 mm laminated silicon iron. Due to the low-duty transient operation a high electrical loading can be used, in order to minimise the weight of the machine. For the same reason a large aspect ratio (stator bore to the machine active length) and peak air gap flux density has been used to meet the maximum torque demand.

TABLE II
PRINCIPAL PARAMETERS OF PROTOTYPE MACHINE DESIGN

No. Poles (p)	No. Slots (q)	Stator Bore (D) (mm)	Active Length (L) (mm)	Air gap (g) (mm)	Airgap flux density (peak) (T)	Electrical Loading (A/m)
16	72	112	35	1	1.25	105000

Based upon the low speed requirements of the machine and the choice of the number of poles, the resulting electrical frequency is relatively low. Because of this the majority of losses generated in the machine are attributed to the winding region. Therefore the choice of conductor, impregnation material and slot liner will have a large impact on the overall thermal performance of the machine. Furthermore the AC losses in the winding can be assumed to be negligible, due to the low operating electrical frequency, the relatively small conductor size and absence of parallel paths. This means that the best course of action to minimise conductor losses is to increase the slot fill factor. A winding arrangement utilising a single large round diameter of Aluminium wire was used, achieving a slot fill factor of 47%. Details of this are presented in Table III and Fig. 1. It was found the use of aluminium wire offered a significant weight benefit in this application.

TABLE III
WINDING CONFIGURATION PARAMETERS

Type	Turns per slot side (N_s)	Throw	Parallel Paths	Path Type	Conductor current density at peak torque (A/mm^2)
Double layer	4	4	1	Upper/ Lower	28.6

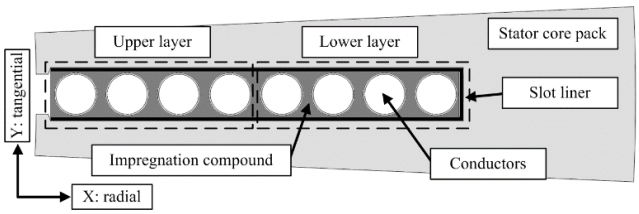

Fig. 1. Outline of a single stator slot together with approximate conductor placement.

III. Motorette Hardware

A. Winding Insulation System

The impregnation materials selected for this investigation are shown in Table IV and Table V. An epoxy potting

compound is chosen for its superior thermal conductivity, superior impregnation goodness within the slot and full encapsulation of the end-winding region, allowing for better heat extraction. Whilst this type of potting material is expected to perform the best, it introduces a more complex impregnation process to the machine manufacture. To balance this two different types of varnish impregnation compounds have been included also. The solvent based varnish is representative of a high temperature system. The non-solvent varnish is a newer impregnation type and offers improved impregnation fill and shorter curing time compared to solvent based systems. Estimations of the varnish impregnation material thermal properties are used [27], as this information is not specified in the manufacturer material data sheets.

TABLE IV
IMPREGNATION COMPOUND PROPERTIES

Property	Elan-tron W 4260 (Epoxylite)	Elmotherm 073-1010 (Elantas)	Elan-protect up 142 (Elantas)
Potting material	Epoxy	Varnish (solvent)	Varnish (non-solvent)
Thermal conductivity (W/m·K)	0.6	≈ 0.13	≈ 0.13
Specific heat capacity (J/kg·K)	1700	≈ 1700	≈ 1700
Density (kg/m^3)	1730	≈ 980	≈ 980
Insulation class	H (180 °C)	N (200 °C)	N (200 °C)

TABLE V
SLOT LINER PROPERTIES

Property	Nomex 410 (Dupont)	ThermaVolt (3M)	PEEK film (VICTREX)
Thickness (mm)	0.18	0.18	0.15
Basis weight (Kg/m^2)	0.174	0.274	-
Dielectric breakdown voltage (kV)	6.12	3.3	18
Tensile strength (kN/m)	22.7/11.6	7.2/3.9	-
Thermal conductivity @ 180°C (W/m·K)	0.143	0.18	0.25
Insulation class	R (220 °C)	R (220 °C)	R (220 °C)

A selection of three different slot liners were also considered in the study. They are all different classes of slot liner material and as such have varying material properties. The PEEK film is a newly available material that offers superior thermal conductivity and dielectric breakdown, showing good potential as a slot liner material. Due to the relatively small slot size of the machine it was desirable to use a thin slot liner material to maximise the slot fill factor. In the initial winding experiments it was found that a 0.18 mm thick liner offered a balance between liner reduction and mechanical rigidity. A 0.18 mm thickness was not available for the PEEK material and such the closest thickness to this was chosen instead (0.15 mm).

B. Motorette Construction

It is not possible to completely replicate the distributed winding configuration in a single tooth motorette. This is because the winding throw is greater than one slot. However for a DC motorette thermal test the volume of conductor present, and associated equivalent power loss is the important component. This means an alternative winding configuration to that of the final machine assembly can be used, as long as the power loss contribution is equivalent.

Motorettes with four slots were constructed for the experiments. This was decided as a compromise between minimising the size of the motorette assembly while ensuring that an end-winding arrangement representative of the final machine assembly could be achieved. A winding pattern using a single phase was derived for simplicity. Fig. 2 shows a comparison between a motorette, and a rapid prototyped stator section of the same shape. The rapid-prototyped stator section has eighteen slots and the central slots of it are wound with three phases in the correct winding pattern required for the complete machine. The motorettes were wound with end-winding lengths that approximate those expected in the complete machine wound stator assembly.

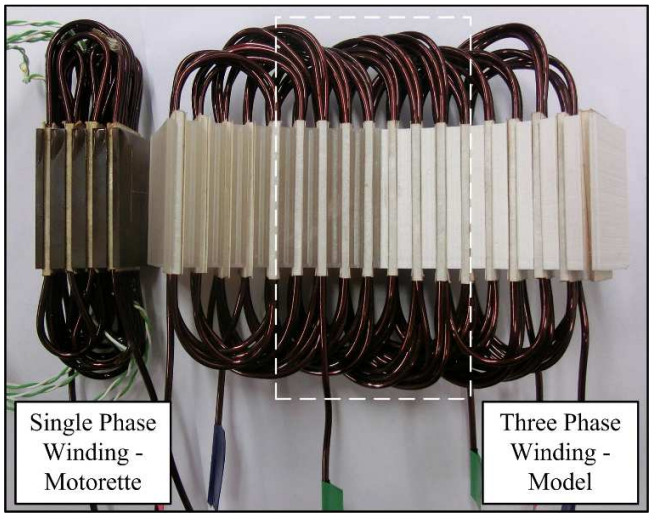

Fig. 2. Motorette (left) with rapid-prototyped stator section model (right)

Nine motorette samples were constructed; three for each impregnation type, each with one of the three slot liners. The winding coil and stator were instrumented with a number of type-K thermocouples located at strategic locations. These include the centre of the slot, end-winding region, centre of the stator tooth, centre of the stator yoke, cold-plate and ambient temperature in the insulated chamber. Two thermocouples were used for each location to introduce a level of redundancy, and also to improve the temperature measurement accuracy by taking an average of the temperature data. Small holes were drilled for the tooth and yoke thermocouples on either side of

the motorette. A high temperature superglue was used to secure the thermocouples in place where necessary, Fig. 3.

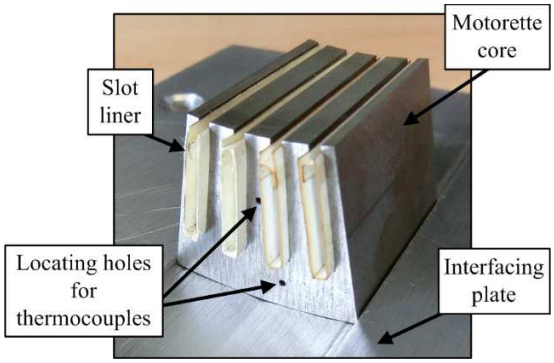

Fig. 3. Motorette before thermocouple instrumentation and impregnation.

Once the motorettes were wound and instrumented with thermocouples they were impregnated with the selected insulation compounds as per the manufacturer instructions. The epoxy resin compound necessitated a mould to allow the end winding region to be fully encapsulated. The varnish based compounds were dipped and baked to cure. A vacuum chamber was used for all motorettes to help remove pockets of air within the sample. Fig. 4 shows all nine motorette samples.

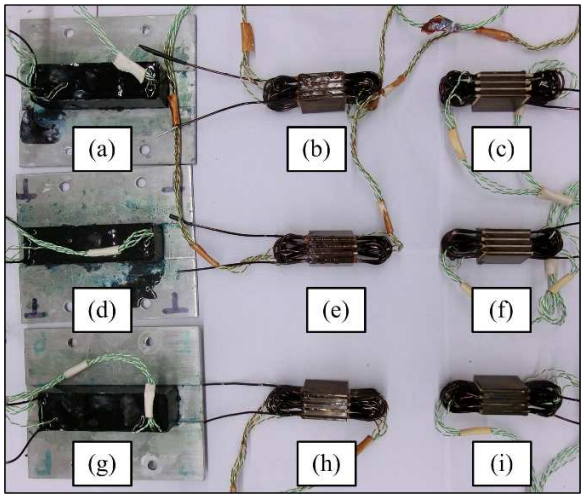

Fig. 4. Motorette samples: epoxy with Nomex liner (a), solvent varnish with Nomex (b), non-solvent varnish with Nomex (c), epoxy with ThermaVolt (d), solvent varnish with ThermaVolt (e), non-solvent varnish with ThermaVolt (f), epoxy with Peek (g), solvent varnish with Peek (h) and non-solvent varnish with Peek (i).

IV. Experimental Setup and Testing Procedure

The experimental setup comprised a thermally insulated chamber, liquid-cooled temperature-controlled cold plate, data acquisition system and dc power supply, Fig. 5. To promote a good contact between the motorette and the flat cold plate an interface plate is used which has one surface machined to the outer stator profile. The interface plate is bolted to the water-cooled cold plate and thermal paste is applied to promote a good interface contact. Similarly thermal paste is applied between the varnish impregnated motorette samples and the interface plate. In addition some external pressure (not shown in Fig. 5), is applied to the top of the varnish impregnated samples to help ensure a good contact between the motorette sample and interface plate. The epoxy impregnated samples however are potted to individual interface plates, and so this additional pressure is not required.

The experiment is set such that the convective heat transfer from the motorette surface, not in contact with the cold plate is negligible [16–21]. Due to the use of the thermally insulated chamber, the water cooled cold plate is the primary means of heat extraction from the sample.

The test profile was controlled using a National Instruments CompactRIO FPGA interfaced to the DC power supply. This allowed a pre-determined duty cycle and accurate timing of the transitions to be programmed.

A consideration when using aluminium conductors is the forming of a good electrical connection as the metal is prone to oxidation when exposed to the environment. A soldering iron with an ultra-sonic vibration attachment was successfully employed to remove oxidation build up while tinning the wire.

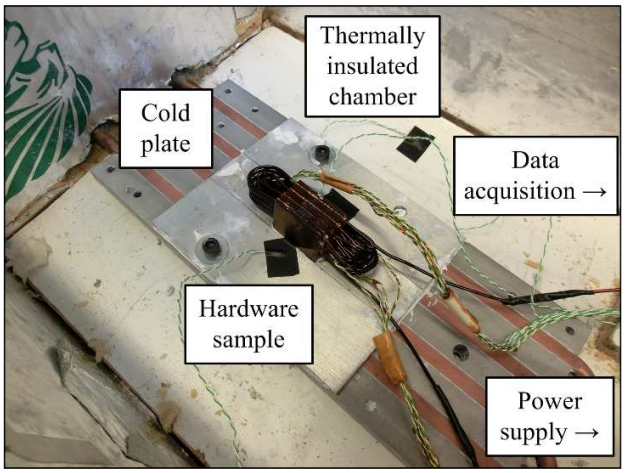

Fig. 5. Experimental setup for DC motorette thermal tests

V. Motorette Results

A. Thermal Steady State

Initially each motorette sample was tested to thermal steady state over a range of DC current/loss values. By monitoring the temperature change for the end-winding region, thermal equilibrium was deemed to be met when the temperature change was less than 1°C over a ten minute period. The current and temperature data for each thermocouple were recorded every ten seconds, and the voltage drop across the motorette sampled at steady state conditions.

The steady state experimental data provides an insight into the power loss handling abilities of the various stator winding sample variants. By evaluating the slot centre temperature rise above the stator back iron the heat transfer capability of the slot region can be deduced. This information for all nine motorette samples has been plotted in Fig. 6. To aid with

comparison Fig. 7 demonstrates the winding loss required to produce a temperature difference of 50°C between the slot centre (winding) and back iron.

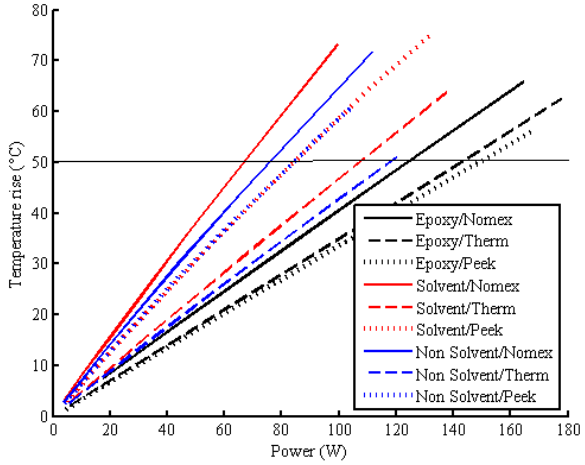

Fig. 6. Slot centre temperature rise above yoke vs. winding dc power loss for motorette variants.

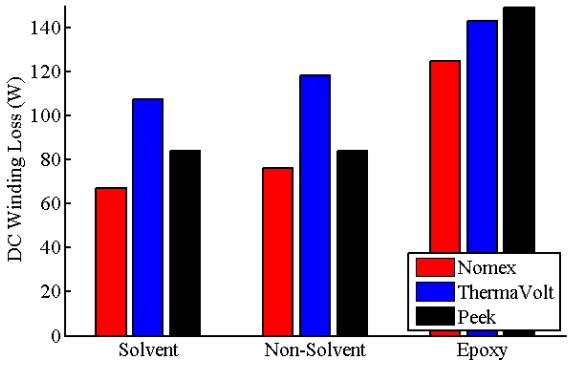

Fig. 7. DC winding loss recorded at a 50°C temperature rise between yoke and slot centre.

As would be expected the epoxy potted motorettes performed better than the varnish potted samples and is a consequence of the higher thermal conductivity of the impregnation material. With the epoxy impregnation an approximately 20% variation in capability exists across the three slot liner materials with PEEK giving the best results, which reflects the differences in the slot liner thermal conductivities. The varnish impregnations however do not follow this trend, where the best performance is obtained with ThermaVolt and the non-solvent varnish system, although the differences between the use of solvent and non-solvent varnishes are not substantial. The ability of the slot liner to absorb the impregnation material improves heat extraction in the slot when combined with varnish based potting compounds. The data suggests that the PEEK plastic has poor porous properties.

B. Thermal Transient Duty Tests

Based upon the experimental results gathered from the steady state thermal tests, two of the most promising configurations were selected for further investigation: non-solvent varnish and ThermaVolt, and epoxy and ThermaVolt. These two motorette samples were tested against the transient duty detailed in Table VI. This is an approximation to the duty seen in the application, but with an extended high output period 'A' to ensure the winding reached a temperature close to, but not exceeding, its rated insulation class. This was necessary due to the improved water-based cooling employed in the motorette experiments.

TABLE VI
MOTORETTE TRANSIENT DUTY CYCLE

Period	Time (secs)	Current (A_{dc})	Ambient Temp. (°C)	Times repeated
A	15	65	25	10
B	45	5	25	

VI. THERMAL MODEL CALIBRATION FOR TRANSIENT DUTY ANALYSIS

A. Motorette thermal model

The results shown in Fig. 6 and Fig. 7 give an initial indication of the thermal conductivity within the slot for the motorette variants. However it is not certain from this data how a full machine assembly would perform, as the cooling, thermal mass and contact between stator and housing will all differ for an actual machine, compared to that of the motorette experimental setup. In order to predict the thermal performance of the full machine assembly a thermal model of the machine should be developed and then calibrated.

A lumped parameter thermal model based on the geometry of the machine, and properties of the materials defined is used [27], Fig. 8. The slot and end-winding regions use a cuboidal element approach, where the winding and impregnation compound are combined into a single component with separate thermal conductivities in three dimensions [28]. The slot region uses two cuboidal elements for the upper/lower parts, Fig. 1, covering the full active length of the machine, i.e. one axial slice. The end-winding region uses a similar arrangement, with upper and lower regions for the front and rear end-winding, totalling four cuboidal elements. The stator tooth is comprised of three temperature nodes: tooth tip, centre and end, with one thermal resistance between them. One temperature node is used for the stator yoke. The housing is composed of three temperature nodes for the active length, front and rear. The thermal contact resistance between slot liner to stator, and stator to housing is modelled as an effective airgap.

Although the rotor and shaft structure is present in the thermal model used, the stator and housing components are isolated to emulate the motorette test setup. This is done by introducing a large scaling factor to all thermal resistances

connecting the stator and rotor. The housing and ambient temperatures are then set to the values recorded from the experimental data to mimic the setup.

Winding losses within the model are calculated based upon the input current and the phase resistance of the winding. The resistance in turn is calculated based upon the specified material parameters, conductor diameter and estimated phase length. Loss scaling with temperature is included.

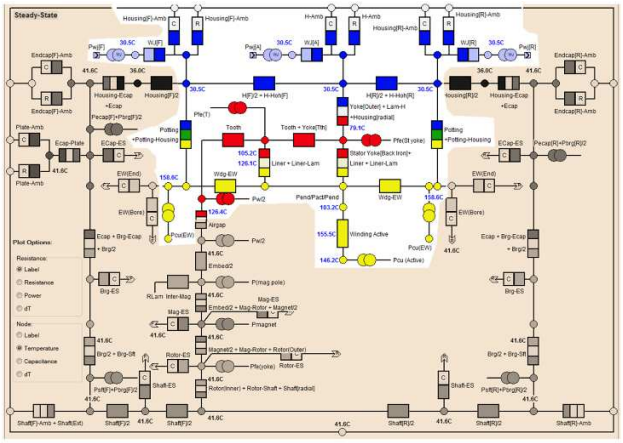

Fig. 8. Lumped parameter thermal model circuit, with stator, slot, end-windings and active section of the housing isolated [27]

B. *Steady state calibration*

A particle swarm optimisation routine [29] and fitness function was developed to calibrate the thermal model for the two chosen motorette variants: non-solvent varnish and ThermaVolt, and epoxy and ThermaVolt. The fitness for each iteration of the calibration process is gauged by how close the model temperature prediction is to that of the motorette steady state data (1). Where T_{mtk} is the recorded temperature data for one of the four regions: slot centre, end-winding, stator tooth or stator back iron, and T_{mdk} is the thermal model prediction for the same region. The fitness is determined as in (2), where a value of one represents a perfect match. Equal weighting is given to the four temperature relative errors, E_k.

$$E_k = \frac{abs(T_{mtk} - T_{mdk})}{T_{mtk}} \quad (1)$$

$$F = 1 - \sum_{k=1}^{4} E_k \quad (2)$$

The eight inputs to the calibration are:

- Radial S_r, tangential S_t and axial S_a thermal conductivity of the slot cuboids.
- Radial EW_r, tangential EW_t and axial EW_a thermal conductivity of the end-winding cuboids.
- Slot liner to stator effective air gap G_{ss}.
- Stator to housing effective air gap G_{sh}.

To aid this process and prevent unrealistic calibration solutions, material test data from [30] is used as a guide. The calibration was carried out using the experimental data from the highest value of current each motorette could handle. Comparisons to the other operating points where then made after the calibration, to gauge the overall effectiveness of the model.

It was important to verify that the estimated losses in the thermal model were close to those recorded from the motorette experiment data. This was done for each recorded steady state point, using the average winding temperature. An under prediction was initially observed, attributed to the estimation for the end-winding length, given that this is the only unknown quantity in calculating the winding phase resistance. A scaling factor of 1.48 was introduced to the model and kept constant throughout the calibration process and full machine assembly prediction.

C. *Transient duty calibration*

Once a good agreement to the steady state data had been achieved, a comparison was then made to the transient thermal experiments. A significant difference between the calibrated model and motorette was initially observed. A sensitivity analysis on the model indicated that the value of thermal capacitance assumed for the impregnation materials was the cause of the discrepancy. The quantity and density of insulating material is determined by the impregnation 'goodness' of the impregnation process. Although it is common to scale the thermal resistance based upon this factor, the thermal capacitance will also be effected, as the actual quantity of impregnation material present in the slot is unknown. Another factor is the lack of accurate material thermal properties, particularly for varnish based impregnation compounds. It is not common for the specific heat capacity or density to be included, as such the properties shown in Table V, which are an estimate.

To calibrate the thermal model to the transient duty, the specific heat capacity of the impregnation compounds were adjusted. Fig. 9 demonstrates a comparison between the transient thermal data recorded from the motorettes, and their corresponding calibrated thermal models for the non-solvent varnish and ThermaVolt motorette. To ease comparison, only the temperatures for the end-winding and yoke regions are shown. It can be seen that a good agreement between the model and motorette data is observed. This process is repeated for the epoxy and ThermaVolt combination, with the calibrated thermal properties displayed for both types shown in Table VII.

The calibrated parameters from Table VII however do not appear to be a physical representation of the system. For example the lower radial S_r, and tangential S_t, thermal conductivity for the epoxy slot cuboidal element compared to the varnish. This is very unlikely given Fig. 6 and Fig. 7. In addition the significant difference in the axial thermal conductivity S_a, between the two samples. Like with most optimisation problems there are multiple good solutions, with the parameters presented in Table VII being just one possible set of these. The motorette experimental data is therefore only useful for predicting the performance of a complete machine, built to the same geometry and using the same active materials as the motorette samples.

It is worth noticing the difference in magnitude of the stator to housing effective airgap G_{sh}, in Table VII. A very low contact resistance was achieved for the epoxy based motorette, likely attributed to the motorette being impregnated to its interface plate, and epoxy resin seeping in and filling the voids in this interface region.

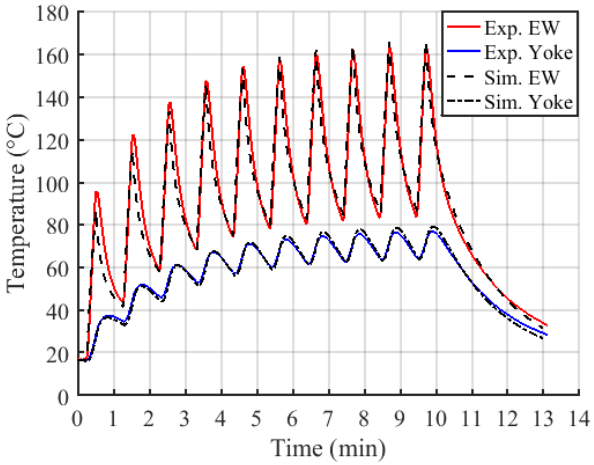

Fig. 9. Calibrated thermal model simulation temperature versus transient motorette experimental data.

TABLE VII
CALIBRATED SLOT THERMAL PROPERTIES

Motorette	Thermal conductivity (W/m·K)						G_{ss} (µm)	G_{sh} (µm)	Impreg. thermal capacitance (J/kg·K)
	S_r (X)	S_t (Y)	S_a (Z)	EW_r (X)	EW_t (Y)	EW_a (Z)			
Epoxy & ThermaVolt	2.80	2.17	255	3.46	1.55	199	2.0	5.0	0.046
NS varnish & ThermaVolt	5.00	4.50	104	2.92	1.38	281	1.9	26.0	0.448

D. Full machine assembly prediction

A prediction of the performance of a full machine assembly, with either insulation combination can be made using these calibrated models. The same slot and winding topology is combined with a V-IPM interior PM rotor, and a radially finned housing for cooling via natural convection. A prediction for the stator to housing thermal interface is made, based upon [31], where an 'average' interface gap of 30 µm is used. In addition the convection coefficient is calculated based on analytical equations [32], based on the geometry of the housing and fins. Fig. 10. shows the thermal predictions of the end-winding temperature when subjected to the transient duty cycle. The duty used is similar to that detailed in Table VI, except with five seconds of high output period 'A', and fifty-five seconds of low output period 'B'. A maximum difference of 50°C is observed by the end of the transient duty, between the two impregnation materials types. However both combinations fall within the maximum insulation class temperature of the winding, and would be sufficient.

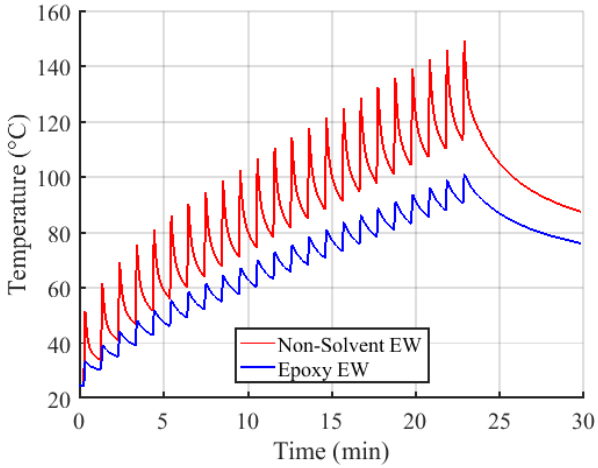

Fig. 10. Predicted end-winding temperature of the full machine assembly with a transient duty.

Based upon the thermal prediction shown in Fig. 10, the non-solvent varnish and ThermaVolt insulation combination was selected for the final machine prototype. A consideration in this selection was the simpler manufacturing process involved with varnish type impregnation. Another less documented factor is the effect of rapid thermal cycling on the impregnation compound, with epoxy potting systems being potentially more vulnerable to thermal expansion, the formation of cracks, and deterioration of the insulation system.

VII. MACHINE PROTOTYPE THERMAL ANALYSIS

The prototype machine was manufactured with the same slot and winding geometry, ThermaVolt slot liner and same brand of non-solvent varnish impregnation compound as the motorette variant. To replicate the same impregnation process as the motorette, the winding was completely submerged in the non-solvent varnish, and placed in a vacuum chamber to vacate pockets of air within the slot. Fig. 11 demonstrates this process, with Fig. 12 showing the winding post-curing. Thermocouples were located in multiple slots, stator teeth and various points on the stator back iron and end-winding region, in both the drive and non-drive ends of the machine. The end-winding length achieved for the real machine was close to that observed in the initial winding trials shown in Fig. 2.

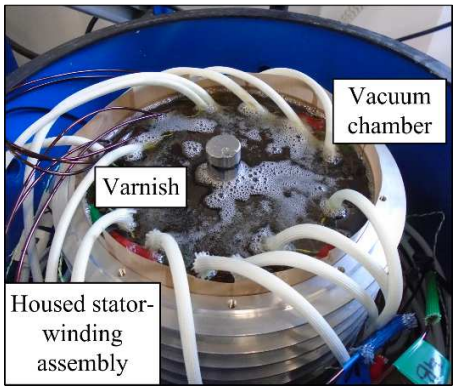

Fig. 11. Impregnating process for complete machine assembly. Winding fully submerged and located in a vacuum chamber.

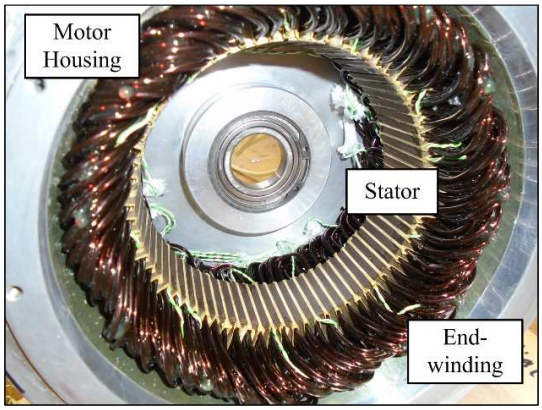

Fig. 12. Stator, housing and winding post-curing of the varnish

Due to the low speed operation of the machine the loss is dominated by winding ohmic effects, with iron loss and stray AC effects small in comparison. For example, the recorded average open-circuit losses at 500 RPM were 18 W, whereas the maximum winding losses are around 5 kW. Consequently the thermal characterisation of the whole machine were carried out using the same DC power supply, and FPGA kit as described in section IV.

The thermal testing on the full prototype stator was initially carried without the inclusion of the rotor and shaft, or mounting arrangement. This was done so as to remove the additional thermal mass associated with these components, in order to simplify the lumped parameter thermal model. Further thermal tests with these components included were also conducted. Fig. 13 shows the initial test setup. Slot liner was placed over each end-cap hole, where the rotor shaft would be located, to minimise any through-draft which may occur due to the absence of the rotor. The testing was carried out with the machine located inside a thermal chamber to maintain a consistent 25°C ambient temperature. Both steady state and transient thermal analysis was carried out, with the temperatures in the slot, end-winding, stator tooth, stator back iron, housing, end-caps recorded alongside the winding power loss. The three phases were connected in series with the DC power supply to ensure balanced losses throughout the machine windings.

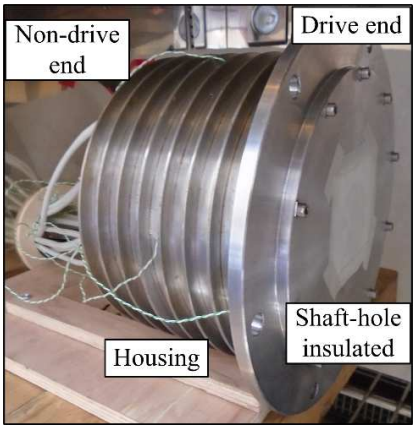

Fig. 13. Stator, housing, winding and end cap assembly placed in a thermal chamber for DC testing.

Fig. 14 compares the thermal prediction made in Fig. 10, with the test data from the full machine assembly, when subjected to the same transient duty. For the purposes of comparison, an early simulation is also included which uses the slot and winding thermal parameters, calculated based on the known material properties presented in Table IV and Table V. In addition, the end-winding scaling factor, introduced after the motorette calibration, is reset to a value of one. A 68°C difference in end-winding temperature is observed between the initial thermal model simulations and the test data. Whereas the prediction made from the motorette calibrated model is much closer with a maximum 12°C difference at the test end.

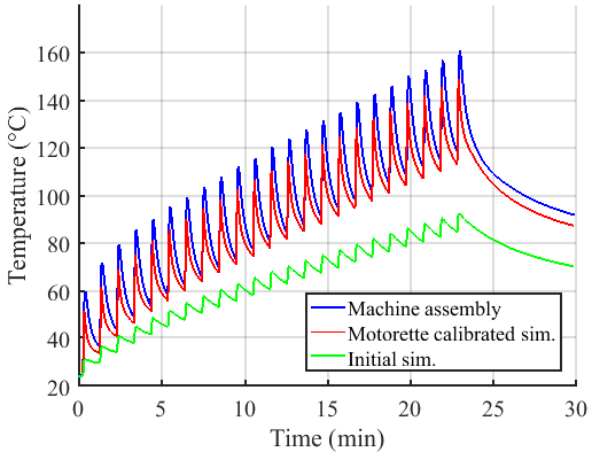

Fig. 14. Average end-winding temperature, recorded machine assembly versus simulation.

Part of this difference can be attributed to the estimation of the winding losses. The experimentally measured and estimated total winding losses between the two thermal models, and the full machine assembly, are compared in Table VIII. This is for a thermal steady state test at 15 A_{rms}. As discussed in section VI-C, an end-winding scaling factor of 1.48 was applied to the motorette calibrated model. It can be

observed this has resulted in a better winding loss prediction, with an accuracy of 90% compared to the full machine assembly. An end-winding scaling factor of 1.7 brings the estimated losses closer to that of the full machine assembly.

TABLE VIII
MEASURED AND SIMULATED STEADY STATE TOTAL WINDING LOSS

Current (A_{rms})	Initial simulation (W)	Motorette calibrated simulation (W)	Machine assembly (W)
15	176	238	266

Fig. 15 plots the transient duty cycle again, except with both models using the same end-winding length, equal to the correct value of the full machine assembly. The model calibrated with the motorette data has a temperature difference of only 0.3 °C by the end of the transient duty, whereas the uncalibrated model under predicts by 35 °C. It can be observed that the slot and winding thermal properties derived from the motorette samples provide an accurate representation of the full machine, even with a small inaccuracy with the end-winding length. Fig. 14 represents the true benefit of performing an experimental calibration, as an under-prediction in the end-winding losses was only observed after experimental testing of the motorettes and final machine prototype. However the motorette calibrated model was significantly closer to the thermal performance of the full machine assembly, compared to simulations made pre-calibration.

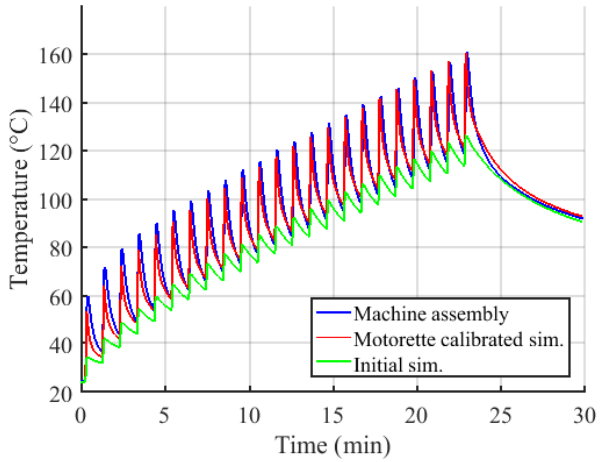

Fig. 15. Average end-winding temperature, recorded machine assembly versus simulation, with identical end-winding length in both simulations.

VIII. CONCLUSIONS

This paper presents an experimental approach to establish an accurate, calibrated thermal model for use in the design of a distributed wound machine for a low-duty transient application. Stator segment (motorette) experiments have been used to provide experimental data to inform and calibrate a lumped parameter circuit model of the machine design.

Used solely for concentrated wound machines so far, a method to develop motorettes for a distributed wound machine has been developed. Based on rapid-prototyped models of the design, estimations of the end-winding length between slots has been found, and a winding layout for a four slot stator segment has been created which mimics the volume of winding in the final machine layout.

Experimental analysis of motorette samples were used to obtain a comparative thermal performance of different impregnation and slot liner insulation systems. The two best variants were selected for more detailed transient thermal analysis. A thermal model, calibrated from steady-state and transient duty tests on the motorettes was used to estimate the thermal performance of the complete machine assembly. The motorette testing identified how the impregnation 'goodness' impacted both the thermal resistance and thermal capacitance of the manufactured winding.

Thermal testing on the corresponding machine prototype demonstrate that accurate thermal parameters of the slot and winding region could be derived from the motorette tests. A small degree of inaccuracy was introduced as a result of a longer end-winding length in the realisation of the distributed winding in the full machine. This could be easily compensated for by scaling an end winding loss.

Overall the experimental calibration approach illustrates the benefit of sub-assembly measurements as a time and cost-effective means for calibrating lumped parameter thermal models used in design of electrical machines, prior to construction of a full machine prototype. The work has shown technique can be effective for a distributing wound machine, and low-duty transient operation.

REFERENCES

[1] A. Boglietti, E. Carpaneto, M. Cossale, A. Lucco Borlera, D. Staton, and M. Popescu, "Electrical machine first order short-time thermal transients model: Measurements and parameters evaluation," in *Industrial Electronics Society, IECON 2014 - 40th Annual Conference of the IEEE*, 2014, pp. 555–561.

[2] Y. K. Chin and D. A. Staton, "Transient thermal analysis using both lumped-circuit approach and finite element method of a permanent magnet traction motor," in *AFRICON, 2004. 7th AFRICON Conference in Africa*, 2004, vol. 2, pp. 1027–1035 Vol.2.

[3] A. M. EL-Refaie, N. C. Harris, T. M. Jahns, and K. M. Rahman, "Thermal analysis of multibarrier interior PM synchronous Machine using lumped parameter model," *IEEE Transactions on Energy Conversion*, vol. 19, pp. 303–309, Jun. 2004.

[4] J. Fan, C. Zhang, Z. Wang, Y. Dong, C. E. Nino, A. R. Tariq, and E. G. Strangas, "Thermal Analysis of Permanent Magnet Motor for the Electric Vehicle Application Considering Driving Duty Cycle," *Magnetics, IEEE Transactions on*, vol. 46, pp. 2493–2496, Jun. 2010.

[5] S. Nategh, Z. Huang, A. Krings, O. Wallmark, and M. Leksell, "Thermal Modeling of Directly Cooled Electric Machines Using Lumped Parameter and Limited CFD Analysis," *IEEE Transactions on Energy Conversion*, vol. 28, pp. 979–990, Dec. 2013.

[6] S. Nategh, O. Wallmark, M. Leksell, and S. Zhao, "Thermal Analysis of a PMaSRM Using Partial FEA and Lumped Parameter Modeling," *Energy Conversion, IEEE Transactions on*, vol. 27, pp. 477–488, Jun. 2012.

[7] N. Rostami, M. R. Feyzi, J. Pyrhonen, A. Parviainen, and M. Niemela, "Lumped-Parameter Thermal Model for Axial Flux Permanent Magnet Machines," *IEEE Transactions on Magnetics*, vol. 49, pp. 1178–1184, Mar. 2013.

[8] T. Sawata and D. Staton, "Thermal modeling of a short-duty motor," in *IECON 2011 - 37th Annual Conference on IEEE Industrial Electronics Society*, 2011, pp. 2054–2059.
[9] A. Boglietti, E. Carpaneto, M. Cossale, and S. Vaschetto, "Stator-Winding Thermal Models for Short-Time Thermal Transients: Definition and Validation," *IEEE Transactions on Industrial Electronics*, vol. 63, pp. 2713–2721, May 2016.
[10] O. I. Okoro, "Steady and transient states thermal analysis of a 7.5-kW squirrel-cage induction machine at rated-load operation," *IEEE Transactions on Energy Conversion*, vol. 20, pp. 730–736, Dec. 2005.
[11] A. Boglietti, A. Cavagnino, and D. Staton, "Determination of Critical Parameters in Electrical Machine Thermal Models," *Industry Applications, IEEE Transactions on*, vol. 44, pp. 1150–1159, 2008.
[12] A. Boglietti, A. Cavagnino, and D. A. Staton, "TEFC induction motors thermal models: a parameter sensitivity analysis," *Industry Applications, IEEE Transactions on*, vol. 41, pp. 756–763, May 2005.
[13] X. Cai, M. Cheng, S. Zhu, and J. Zhang, "Thermal Modeling of Flux-Switching Permanent-Magnet Machines Considering Anisotropic Conductivity and Thermal Contact Resistance," *IEEE Transactions on Industrial Electronics*, vol. 63, pp. 3355–3365, Jun. 2016.
[14] R. Camilleri, D. A. Howey, and M. D. McCulloch, "Experimental investigation of the thermal contact resistance in shrink fit assemblies with relevance to electrical machines," in *Power Electronics, Machines and Drives (PEMD 2014), 7th IET International Conference on*, 2014, pp. 1–9.
[15] G. G. Guemo, P. Chantrenne, and J. Jac, "Parameter identification of a lumped parameter thermal model for a permanent magnet synchronous machine," in *Electric Machines Drives Conference (IEMDC), 2013 IEEE International*, 2013, pp. 1316–1320.
[16] S. Ayat, R. Wrobel, J. Goss, and D. Drury, "Experiment Informed Methodology for Thermal Design of PM Machines," in *Ecological Vehicles and Renewable Energies (EVER), 2016 Eleventh International Conference on*, 2016.
[17] J. L. Baker, R. Wrobel, D. Drury, and P. H. Mellor, "A methodology for predicting the thermal behaviour of modular-wound electrical machines," in *Energy Conversion Congress and Exposition (ECCE), 2014 IEEE*, 2014, pp. 5176–5183.
[18] R. Wrobel, P. H. Mellor, and D. Holliday, "Thermal Modeling of a Segmented Stator Winding Design," *Industry Applications, IEEE Transactions on*, vol. 47, pp. 2023–2030, 2011.
[19] R. Wrobel, A. Mlot, and P. H. Mellor, "Investigation of end-winding proximity losses in electromagnetic devices," in *Electrical Machines (ICEM), 2010 XIX International Conference on*, 2010, pp. 1–6.
[20] R. Wrobel, D. Salt, N. Simpson, and P. H. Mellor, "Comparative study of copper and aluminium conductors - Future cost effective PM machines," in *Power Electronics, Machines and Drives (PEMD 2014), 7th IET International Conference on*, 2014, pp. 1–6.
[21] R. Wrobel, D. Staton, R. Lock, J. Booker, and D. Drury, "Winding Design for Minimum Power Loss and Low-Cost Manufacture in Application to Fixed-Speed PM Generator," *Industry Applications, IEEE Transactions on*, vol. 51, pp. 3773–3782, 2015.
[22] J. Richnow, P. Stenzel, A. Renner, D. Gerling, and C. Endisch, "Influence of different impregnation methods and resins on thermal behavior and lifetime of electrical stators," in *Electric Drives Production Conference (EDPC), 2014 4th International*, 2014, pp. 1–7.
[23] R. Wrobel, S. J. Williamson, J. D. Booker, and P. H. Mellor, "Characterising the performance of selected electrical machine insulation systems," in *Energy Conversion Congress and Exposition (ECCE), 2015 IEEE*, 2015, pp. 4857–4864.
[24] J. Godbehere, R. Wrobel, D. Drury, and P. H. Mellor, "Design methodology of a brushless IPM machine for a zero-speed injection based sensorless control," in *Energy Conversion Congress and Exposition (ECCE), 2015 IEEE*, 2015, pp. 5601–5608.
[25] J. Godbehere, R. Wrobel, D. Drury, and P. H. Mellor, "Salient PM rotor topology selection for a zero-speed injection based sensorless controlled machine," in *8th IET International Conference on Power Electronics, Machines and Drives (PEMD 2016)*, 2016, pp. 1–6.
[26] J. Godbehere, R. Wrobel, D. Drury, and P. H. Mellor, "Experimentally calibrated thermal stator modelling of AC machines for short-duty transient operation," in *2016 XXII International Conference on Electrical Machines (ICEM)*, 2016, pp. 1721–1727.
[27] Motor-CAD, "http://www.motor-design.com."
[28] R. Wrobel and P. H. Mellor, "A General Cuboidal Element for Three-Dimensional Thermal Modelling," *Magnetics, IEEE Transactions on*, vol. 46, pp. 3197–3200, 2010.
[29] J. Robinson and Y. Rahmat-Samii, "Particle swarm optimization in electromagnetics," *Antennas and Propagation, IEEE Transactions on*, vol. 52, pp. 397–407, Feb. 2004.
[30] N. Simpson, R. Wrobel, and P. H. Mellor, "Estimation of Equivalent Thermal Parameters of Impregnated Electrical Windings," *Industry Applications, IEEE Transactions on*, vol. 49, pp. 2505–2515, Nov. 2013.
[31] D. Staton, A. Boglietti, and A. Cavagnino, "Solving the More Difficult Aspects of Electric Motor Thermal Analysis in Small and Medium Size Industrial Induction Motors," *Energy Conversion, IEEE Transactions on*, vol. 20, pp. 620–628, 2005.
[32] D. A. Staton and A. Cavagnino, "Convection Heat Transfer and Flow Calculations Suitable for Electric Machines Thermal Models," *Industrial Electronics, IEEE Transactions on*, vol. 55, pp. 3509–3516, Oct. 2008.